

# Numerical Discretizations Via Totally Volume Integrals Discontinuous-Galerkin Method (TVI-DG) for Non-Conventional $[0 \pi]$ Interval

Elhadi I. Elhadi

Department of Mechanical Engineering  
University of Benghazi  
Benghazi, Libya  
Elhadi\_elhadi@yahoo.com

Ahmed Ballil

Department of Mechanical Engineering  
University of Benghazi  
Benghazi, Libya  
Ahmed.ballil @uob.edu.ly

**Abstract**— It is well known that the Discontinuous-Galerkin method (DGM) is an effective numerical method for space discretization, and the approach has advanced rapidly in recent years. This work aims to investigate the shape functions for an interval other than the standard or traditional  $[0 1]$  or  $[-1 1]$ , where this paper is part of a series of papers. The shape function for the non-standard interval  $[0 \pi]$  is investigated for both the space and time discretizations. The numerical results demonstrated that the order of accuracy of the shape functions constructed from polynomials within the interval  $[0 \pi]$  is satisfied. The comparison between the shape function of this work and one for the conventional  $[0 1]$  interval shows that the equivalence in the numerical results is achieved at time  $t = \pi$ . The findings clearly illustrate the adaptability and efficiency of the TVI-DG method in tackling the numerical solution for non-conventional intervals.

**Keywords**—Space and Time Discretizations; Discontinuous-Galerkin Method (DGM); Totally Volume Integrals (TVI); Non-conventional Interval.

## I. INTRODUCTION AND BACKGROUND

It is well recognized that the Discontinuous-Galerkin method (DGM) is a potent numerical method for space discretization. The method has experienced swift development in recent years. It has rapidly been applied in a wide range of applications, including unsteady turbulent flows, continuum mechanics, turbomachinery, chemically reacting flows, and combustion [1], [2], and [3].

As an example of numerical development methods, a discontinuous Galerkin volume integral equation approach was introduced for the analysis of scattering phenomena involving inhomogeneous objects in [4]. It was demonstrated that the developed approach has various advantages over conventional volume integral techniques, and the findings confirmed the correctness and efficiency of the suggested method.

A novel approach called the totally volume integral discontinuous Galerkin method (TVI-DG) was introduced in [5]. This developed technique is based on transforming the boundary integrals into the volume integrals. The method was tested for accuracy using the one-dimensional unsteady linear convection equation, inviscid Burger's equation, and Buckley-Leverett equation. The numerical results showed that the approach is highly efficient for the considered hyperbolic conservation equations.

A totally volume integral of the local discontinuous Galerkin (TV-LDG) method was developed for solving the time-dependent linear convection diffusion equation in [6]. In space, the equation was numerically discretized using the local discontinuous Galerkin method, with boundary integrals transformed into volume integrals. The time discretization was achieved using the third-order explicit strong stability preserving Runge-Kutta (3,3) method. The numerical results demonstrated that the developed scheme is very efficient to solve the unsteady linear advection-diffusion equation in one- and two-dimensional domains.

Recently, Elhadi et al. [7] extended a procedure for solving 2D Euler equations on Cartesian coordinates. The method was based on a high-order precise totally volume Galerkin discontinuous finite element method (TVI-DG). The divergence theorem was used to translate the boundary integral of the Riemann fluxes into volume integrals, where the accuracy is not affected by the border integral fluxes at the element boundaries. The precision was achieved by using high-order polynomial approximations within elements via the tensor product of Lagrange polynomials. The strong stability-preserving Runge-Kutta method SSPRK (3, 3) is used for temporal integration, and the technique was stabilized via the Streamline Upwind Petrov Galerkin (SUPG) stabilization scheme. The results showed that the scheme clearly describes the solution's behavior with all details. Furthermore, the developed TVI-DG was computationally faster than the standard nodal discontinuous Galerkin method.

While all previous research works were applied on the conventional intervals  $[0, 1]$  or  $[-1, 1]$ , this contribution aims to investigate the shape function for the non-conventional interval  $[0, \pi]$  for both the space and time discretizations. We organize the remainder of the paper as follows: The methodology is presented in the next section, where the second- and third-order spatial discretization of the TVI-DG methods for  $\pi$  intervals are introduced. Also, the second- and third-order strong stability-preserving time discretization methods (SSP) for  $\pi$  intervals are presented in the same section. The numerical results are presented in section (III), and the concluding remarks are presented in section (IV).

## II. METHODOLOGY

### A. The Mathematical Formulation and Numerical Discretization

In order to obtain the numerical solution of hyperbolic conservation laws

$$u_t + F(u)_x = 0 \quad (1)$$

where  $u(x, t)$  is the conservative variable and  $F(u)$  is the conservative flux. The numerical solution is complicated by the fact that the solution may develop discontinuities. For this reason, significant effort has been expended on finding spatial discretizations that can handle discontinuities [8]. So, the target is to find a numerical approximation that discretizes the spatial derivative term. Once the spatial derivative is discretized, the obtained is a system of ordinary differential equations (ODEs) in time variable [9]. Thus, the semi-discrete scheme in time can be written as

$$u_t = -Lu \quad (2)$$

where  $Lu$  is the spatial discretization of the function  $u$ . Note that, however, the function  $u$  is a function of both space and time,  $u(x, t)$ , so the semi-discretization is permissible to separate it into  $u(x)$  alone and  $u(t)$ . Most researchers discretized the functions  $u(x)$  and  $u(t)$  by using Legendre or Chebyshev polynomials within intervals  $[-1, 1]$  or  $[0, 1]$ . However, these polynomials are special cases of the Jacobi polynomial. There are many polynomials like the Laguerre polynomial for the interval  $[0, \infty]$ , the Hermite polynomial for the interval  $[-\infty, \infty]$ , and the simple harmonic oscillator  $[0, 2\pi]$ . Therefore, this work can be divided into a series of papers. Each paper is concerned with a certain interval. In this paper, we are concerned with a polynomial that is useful for the interval  $[0, \pi]$ . Where the general Fourier series theory is allowed to write a function  $u(x)$  or  $u(t)$  as a linear combination of an orthogonal system of functions as follows [10], [11]:

$$u(x) = \sum_{n=0}^{\infty} c_n \phi_n \quad (3)$$

This set of real-valued functions is orthogonal with respect to a weight function  $w(x)$  on an interval  $[a, b]$ . If the set is orthogonal, then

$$\int_a^b w(x) \phi_m(x) \phi_n(x) dx = 0 \quad \text{if } m \neq n \quad (4a)$$

and

$$\int_a^b w(x) \phi_m(x) \phi_n(x) dx = 1 \quad \text{if } m = n \quad (4b)$$

The coefficients of the set can be determined by:

$$c_n = \frac{\int_a^b w(x) u(x) \phi_n(x) dx}{\|\phi_n\|^2} \quad (5)$$

Let us name  $w(x)$  and  $w(t)$  as polynomial weighting functions to distinguish them from the governing equation weighting functions  $W(x)$  and  $W(t)$ .

### B. TVI-DG Spatial Discretization In Interval $[0, \pi]$

For a clear explanation, a review of discontinuous Galerkin semi-discretized for solving partial differential equations (PDE) is presented in this section.

Consider the one-dimensional conservation law equation:

$$\frac{\partial u}{\partial t} + \frac{\partial F(u)}{\partial x} = 0$$

The numerical solution of (6) is sought in the computational domain  $\Omega$ , subject to proper initial and boundary conditions. The weighted residual formulation can be accomplished by multiplying (6) by the weighting or test function of the  $x$ -variable  $W(x)$  and integrating by parts over the domain:

$$\int_{\Omega} [W(x) u_t - W_x F(u)] d\Omega + \int_{\Gamma} [F(u) \cdot W(x)] \cdot n d\Gamma = 0 \quad (7)$$

where  $\Gamma$  is the boundary

Subdivided the computational domain  $\Omega$  into  $N$  non-overlapping elements:

$$\Omega = \sum_{h=1}^N \Omega_h \quad (8)$$

$$\int_{\Omega_h} [W_h(x) u_t - W_x F(u_h)] d\Omega_h + \int_{\Gamma_h} [F_b(u_h) \cdot W_h(x)] \cdot n d\Gamma_h = 0 \quad (9)$$

where  $W_h(x)$  and  $F(u_h)$  are the weighting and flux functions over the element domain and  $F_b(u)$  is the flux over the element boundaries. For the sake of simplicity, let us eliminate the element subscript ( $h$ ) and, by applying the divergence theory to the last term of (9), get

$$\int_{\Omega} W u_t - \frac{\partial W}{\partial x} F(u) + (W \frac{\partial}{\partial x} + (\frac{\partial W}{\partial x})) F_b d\Omega = 0 \quad (10)$$

This is the totally volume discontinuous Glerken method (TVI-DG) method [5].

where in this work, the element domain  $\Omega = [0, \pi]$  or  $(a = 0 \text{ and } b = \pi)$ ,  $w(x) = 1$ , with  $u(x) = W(x)$  for the standard Galerkin method; otherwise, it is the petrov-Galerkin method. On the other hand, we have  $\phi_0 = 1$  and  $\phi_1 = x$  for the second-order shape and weight functions and  $\phi_2 = x^2$  for the third-order functions,

then substitution into equations (3) to (5) gives the complete spatial discretization.

### C. Strong Stability Preserving (SSP)-Time Discretization in Interval $[0, \pi]$

Once the spatial discretization is completed, let the spatial part of (10) into the right. Then multiplying the equation by  $W(t)$  and integrating over the time domain  $\Omega = [0, \pi]$  yields:

$$\int_{\Omega} W(t) Q_t = W(t) Lu \quad (11)$$

where  $Q_t = W(x) \frac{\partial u}{\partial t}$ ,  $Lu$  represents the spatial discretization of the  $u$  function, which remains constant over time. where in this paper the time function  $u(t)$  and weight function  $W(t)$  over the domain  $\Omega = [0, \pi]$  with  $\phi_0 = 1$  and  $\phi_1 = t$  for the second-order shape function and  $\phi_2 = t^2$  for the third-order function, and then substitution into equations (3) to (5).

After manipulations, the second-order SSP time discretizations for the  $[0, \pi]$  interval are given as:

For completeness, let  $u^n = Q^n$

$$u^0 = u^n$$

Step (1)

$$u^1 = u^0 + 3.1415926535924141305 Lu^0 \Delta t$$

Step (2)

$$u^2 = u^0 + 1.57079632679850655 Lu^0 \Delta t + 1.57079632679850655 Lu^1 \Delta t \quad (12)$$

where  $Lu^n$  is the spatial discretization at step  $n$  and  $\Delta t$  is the time step,  $n = 0, 1, 2$ ,

The third order SSP-time discretizations for the  $[0, \pi]$  interval are given as:

$$u^0 = u^n$$

Step (1)

$$u^2 = u^0 + 3.14159265358979323846 Lu^0 \Delta t$$

where  $u^2$  as a guess value

$$u^1 = 0.75 u^0 + 0.25 u^2 + 0.785398163398 Lu^0$$

Step (2)

$$u^2 = u^0 + 3.141592653592 Lu^1 \Delta t$$

Step (3)

$$u^3 = u^0 + 0.523598775599 Lu^0 + 2.094395102398 Lu^1 + 0.523598775595 Lu^2 \quad (13)$$

The Courant number is equal to unity for both the second and third SSP-time methods.

For the purpose of comparison, the standard SSP-time method is given as

$$u^0 = u^n$$

Step (1)

$$u^1 = u^0 + Lu^0 \Delta t$$

Step (2)

$$u^2 = u^0 + (0.5Lu^0 + 0.5Lu^1) \Delta t \quad (14)$$

### III. TEST CASES AND NUMERICAL RESULTS

In this manuscript, we examine the same test examples utilized in the first paper [12] of our series for the purpose of comparison, where the totally volume-discontinuous Galerkin is employed. The code was developed in C++ and compiled using g++. All computations were conducted on an HP laptop featuring an Intel® Core™ i7-10510U processor, operating at 1.80 GHz and 2.30 GHz, with 8 GB of memory. The system ran on the Ubuntu 24.04 LTS Linux operating system.

The global error is calculated as the difference between the exact solutions and the numerical solutions. The discretized  $L_1$  norm error is given as

$$L_1 = \sum_{i=1}^N (u_{\Sigma_{edof}^{ex}} - u_i) / tdof$$

where  $N$  is the total degree of freedom,  $edof$  is the element degree of freedom, and  $tdof$  is the total degree of freedom ( $N \times edof$ ).

#### A. Test Example (1)

The first test example is the linear advection equation, considered in many references such as [13] and [14].

$$\left( \frac{\partial u}{\partial t} \right) + \frac{\partial F(u)}{\partial x} = 0$$

where  $F(u) = u$ , the initial condition is given as  $\sin(x)$  with periodical boundary conditions.

The problem domain  $[-\pi, \pi]$  is divided into  $N$  equally spaced elements. The approximate solutions are constructed from polynomials of order 2 and 3, with an interval of  $[0, \pi]$ . In addition to that, SSP-time discretizations of order 2 and 3 are given in (12) and (13), which are used for time evaluation. The exact solution is given as  $u(x, t) = \sin(x - t)$ .

Fig.1 displays the numerical and the exact solutions at time  $t = 1$ , and Fig. 2 shows the  $L_1$  error of

polynomials of orders  $K = 2$  and  $K = 3$  for the 1D linear advection equation test. The order of accuracy and  $L_1$  error are demonstrated in Tables (I) and (II) for polynomials of order  $k = 2$  and 3, respectively.

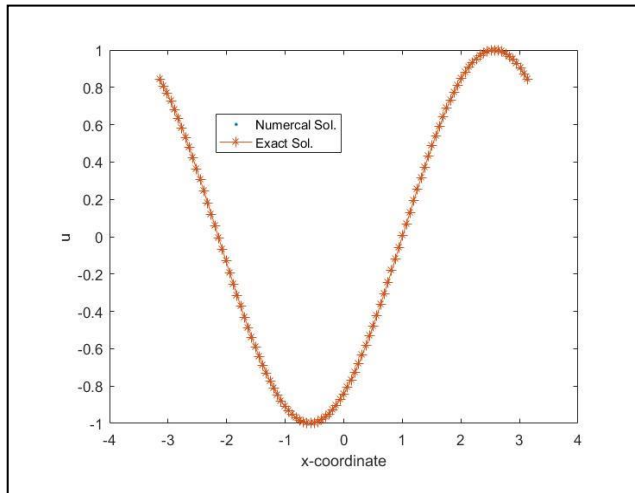


Fig. 1. The numerical and exact solutions of the linear advection equation at time  $t = 1$ .

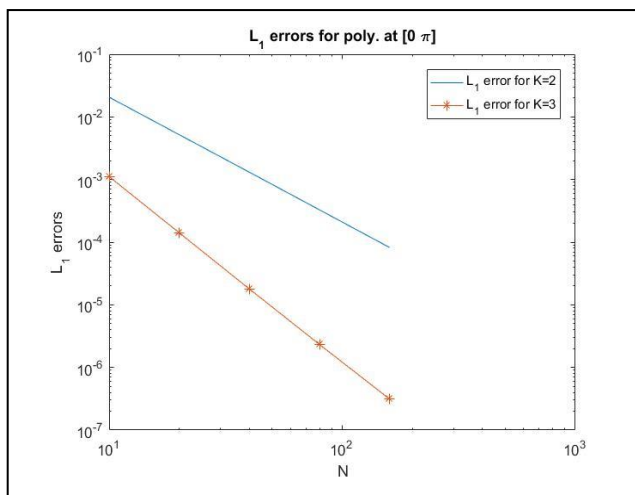


Fig. 2.  $L_1$  error of polynomials of orders  $K=2$  and  $K=3$  for the 1D linear advection equation test.

TABLE I. THE ORDER OF ACCURACY AND  $L_1$  ERROR OF LINEAR ADVECTION EQUATION AT TIME  $T=1$  FOR POLYNOMIAL OF ORDER  $K=2$ .

Number of elements (N)	$L_1$ error	$L_1$ order of accuracy
10	2.05955750001081e-02	-
20	5.18448555568298e-03	1.990062
40	1.30542589281415e-03	1.989680
80	3.27096281698599e-04	1.996733
160	8.17976632966066e-05	1.999584

TABLE II. THE ORDER OF ACCURACY AND  $L_1$  ERROR OF LINEAR ADVECTION EQUATION AT TIME  $T=1$  FOR POLYNOMIAL OF ORDER  $K=3$ .

Number of elements (N)	$L_1$ error	$L_1$ order of accuracy
10	1.11286305377036e-03	-
20	1.40721184981305e-04	2.983365
40	1.78297525500223e-05	2.980481
80	2.31489072452643e-06	2.945271
160	3.10900278812813e-07	2.896420

### B. Test Example (2)

The second test example is a one-dimensional heat equation (1D diffusion equation), which was utilized widely in literature as a benchmark test, for example in [6] and [15].

The governing equation is given as

$$\frac{\partial u}{\partial t} = \frac{\partial^2 u}{\partial x^2}$$

The equation is subjected to initial and boundary conditions and is given as:

$$u(0, x) = \sin(x), \quad u(0, t) = u(\pi, t) = 0$$

The computational domain  $[-\pi, \pi]$  is divided into  $N=40$  equally spaced elements. The numerical solution starts by reducing the second-order partial differential equation into two first-order differential equations (local discontinuous Galerkin method) as follows:

Let  $Q = \frac{\partial u}{\partial x}$  and  $\frac{\partial u}{\partial t} = \frac{\partial Q}{\partial x}$ . These two equations can be solved numerically.

Fig. 3 presents the comparison between the numerical solutions of shape functions by polynomials at intervals  $[0, \pi]$  and  $[0, 1]$  of order  $K = 2$ , at times  $t = 0.5$  and 1. The figure shows that as time increases, the top points decrease, whereas for the standard polynomial  $[0, 1]$ , the numerical data and figure show that the top values are 0.605531 and 0.367076 for the standard interval, respectively. While for  $[0, \pi]$ , the top values at time  $t = 0.5$  and 1 are 0.852037 and 0.726688, respectively. Finally, at time  $t = \pi$ , the maximum value is 0.369835, which is equivalent to the value of the standard polynomial at time  $t = 1$ .



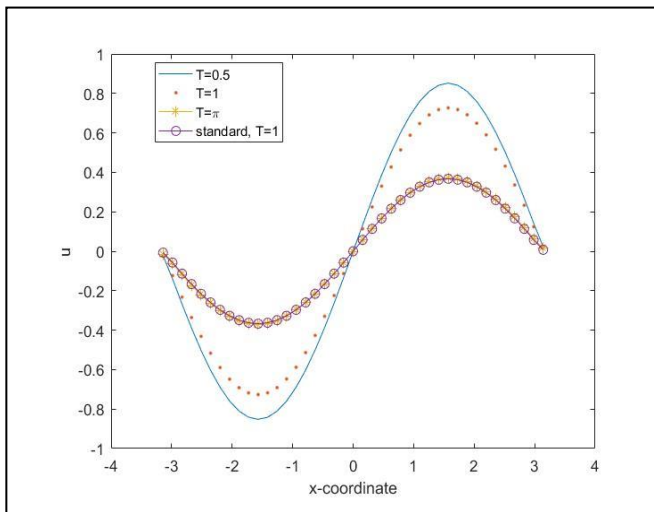


Fig. 3. The comparison between numerical solutions of the  $\sin(x)$  1D heat equation at intervals  $[0, \pi]$  and  $[0, 1]$ .

#### IV. CONCLUSIONS

In this work, two space shape functions of order  $K = 2$  and  $3$  are introduced in addition to those two SSP-time dependent methods, also of order  $K = 2$  and  $K = 3$ , all of them at the non-conventional interval  $[0, \pi]$ . The linear advection equation test example is used to investigate the order of accuracy of both space and time shape functions for  $[0, \pi]$  interval. The numerical results indicate that the shape functions developed from polynomials in the interval  $[0, \pi]$  reach the anticipated level of accuracy. The numerical solution of the heat equation test showed that as time increases, the top values of the numerical solutions decay. The comparison with the standard interval  $[0, 1]$  showed that the numerical values at time  $t = \pi$  are equivalent to time  $t = 1$  for the standard polynomial. To advance this research, additional studies will explore the discretization of the polynomial in both space and time across various non-conventional intervals, utilizing the same test examples for comparison.

#### REFERENCES

- [1] F. Hindenlang, G. J. Gassner, C. Altmann, A. Beck, M. Staudenmaier, and C. D. Munz, "Explicit discontinuous Galerkin methods for unsteady problems," *Computers & Fluids*, Vol. 61, pp 86-93, 2012.
- [2] N.C. Nguyen, and J. Peraire, "Hybridizable discontinuous Galerkin methods for partial differential equations in continuum mechanics," *Journal of Computational Physics*, vol. 231(18), pp 5955-5988, 2012.
- [3] Yu Lv, and M. Ihme, "Discontinuous Galerkin method for multicomponent chemically reacting flows and combustion," *Journal of Computational Physics*, vol. 270, pp. 105-137, 2014.
- [4] Li-M. Zhang, X. Q. Sheng, "A discontinuous Galerkin volume integral equation method for scattering from inhomogeneous objects," *IEEE Transactions on Antennas and Propagation*, vol.63(12), pp 5661-5667, December 2015.
- [5] I. M. Rustum, and E. I. Elhadi, "Totally volume integral of fluxes for discontinuous Galerkin method (TVI-DG) I- unsteady scalar one dimensional conservation laws," *Al-Mukhtar Journal of Sciences*, Vol. 32(1), pp 36-45, 2017.
- [6] E. I. Elhadi, M. A. Fakroon, and A. A. Buzghaiba, "Solving the unsteady linear advection diffusion equations by using the totally volume integral of the local discontinuous Galerkin method," *Libyan Journal of Science & Technology*, Vol. 11(1), pp 53-60, 2020.
- [7] E. I. Elhadi, A. A. Buzghaiba, and M. A. Fakroon, "Totally volume integral of fluxes for discontinuous Galerkin method-two dimensional Euler equations," *Libyan Journal of Science & Technology*, Vol. 13(2), pp 91-96, 2021.
- [8] S. Gottlieb, D. Ketcheson and C. W. Shu, "Strong Stability Preserving Runge-Kutta and Multistep Time Discretizations" World Scientific Press, 2011.
- [9] S. Gottlieb and S. J. Ruuth, "Optimal strong-stability-preserving time stepping schemes with fast downwind spatial discretizations," *Journal of Scientific Computing*, Vol. 27, pp. 289-303, 2006.
- [10] G. B. Arfken and H. J. Weber, "Mathematical Methods for Physicists," 6th Edition, Elsevier, 2005.
- [11] A. Jeffrey and H. H. Dai, "Handbook of Mathematical Formulas and Integrals," 4th Edition. Academic Press, Elsevier 2008.
- [12] E. I. Elhadi, A. A. Abdalla, and E. A. Alabeedy, "Spatial and temporal discretizations using totally volume integrals discontinuous-Galerkin methods: application to non-standard interval  $[0, \sqrt{\pi}]$ ," *International Journal of Aerospace and Mechanical Engineering*, WASET, Vol. 19(5), pp 88-91, 2025.
- [13] G. S. Jiang and C. W. Shu "Efficient implementation of weighted ENO schemes," *Journal of Computational Physics*. Vol. 126, pp 202-228, 1996.
- [14] J. E. Flaherty, L. Krivodonova, J-F. Remacle and M. S. Shephard, "Aspects of discontinuous Galerkin methods for hyperbolic conservation laws" *Journal of Finite Elements in Analysis and Design*. Vol. 38, pp 889-908, 2002.
- [15] R. M. Kirby and G. E. Karniadakis, "Selecting the numerical flux in discontinuous-Galerkin methods for diffusion problems" *Journal of Scientific computing*, Vol. 22, pp 385-411, June (2005).